Chemical Engineering Communications
Publication details, including instructions for authors and subscription information:
http://www.informaworld.com/smpp/title~content=t713454788

ON FLOW LENGTH REQUIREMENT FOR STRESS-INDUCED POLYMER MIGRATION IN FINE CAPILLARIES

A. Dutta[a]; D. D. Ravetkar[a]; R. A. Mashelkar[a]
[a] Chemical Engineering Division, National Chemical Laboratory, Pune, India

To cite this Article Dutta, A. , Ravetkar, D. D. and Mashelkar, R. A.(1987) 'ON FLOW LENGTH REQUIREMENT FOR STRESS-INDUCED POLYMER MIGRATION IN FINE CAPILLARIES', Chemical Engineering Communications, 53: 1, 131 — 147
To link to this Article: DOI: 10.1080/00986448708911888
URL: http://dx.doi.org/10.1080/00986448708911888

Chem. Eng. Comm. 1987, vol 53, pp. 131–147
Photocopying permitted by license only

Printed in the United States of America

ON FLOW LENGTH REQUIREMENT FOR STRESS-INDUCED POLYMER MIGRATION IN FINE CAPILLARIES†

A. DUTTA, D.D. RAVETKAR and R.A. MASHELKAR

Chemical Engineering Division
National Chemical Laboratory
Pune 411 008, India

(Received February 4, 1986; in final form August 21, 1986)

The development of macromolecular concentration gradient caused by the stress induced migration phenomenon in capillary flows has been studied numerically. It is shown that for reaching a given level of flow enhancement, the capillary lengths required are considerably less than those expected from prior analyses, which have neglected the strong interdependence between the flow field and the resulting concentration profiles. The implications of the present findings in terms of detection of macromolecular migration in capillary flows and also the influence on transport rates have been discussed critically.

INTRODUCTION

Art Metzner's research efforts spanning over the past three decades have had enormous impact on the development of the field of non-Newtonian fluids engineering. His unusual analytical mind and his sharp and incisive approach to the solution of problems has led to so many pioneering contributions and opened up so many new vistas in this field. He has influenced the development of the field and equally importantly, he has influenced so many scientists around the world in a profound way and this includes one of us (RAM). This contribution has really originated out of yet another of Art's inspiring thoughts that he projected about 8 years ago. It is a pleasure to dedicate this contribution to him on the occasion of his 60th birthday.

We are concerned with the flows of polymer solutions through very fine capillaries and in thin falling films, which show some peculiarities. Conventional theories which assume no slip at the wall in such cases and flow enhancement over what is predicted by such theories is observed [1–13]. It is believed that flow enhancement is most likely to be due to the migration of polymer molecules away from the wall. Presently, however, the precise cause of this migration phenomenon is not clear and several different hypotheses have been proposed.

Some intuitively appealing thermodynamic arguments were advanced by Metzner [14], which enabled the development of a quantitative framework for

† NCL Communication No. 3977.

analysing migration phenomena. Elaborate quantifications have appeared in the literature over the past few years [15–18]. These workers essentially attribute the phenomenon of polymer migration to the changes in entropy arising out of the deformation of molecules. The essence of the proposed hypothesis is that in a deforming fluid the macromolecules become aligned and stretched thus creating spatial variation of deformation rate. The entropy and hence the free energy also becomes position dependent. In order to compensate for the spatial variation in free energy levels, concentration gradients are induced. The net effect is that polymer molecules migrate towards regions of lower stress levels. Consequently, a polymer depleted low-viscosity layer is formed in the high shear regions adjacent to the wall and the bulk of the high viscosity core liquid 'appears' to slip through this wall layer. Although the validity of the above thermodynamical arguments has been questioned by Tirrell and coworkers [19, 20], a theoretical justification has been recently provided by Cohen and Metzner [18, 21] by using a thermomechanical theory of mixtures. An alternative treatment based on an internal variable thermodynamic theory reported by Drout and Maugin [22] also serves as a theoretical basis for the above arguments.

The key question pertaining to the above mechanistic interpretation is concerned with the order of flow lengths (or times) necessary for the migration to be appreciable. Tirrell and Malone [14] presented an approximate analysis of flow-induced migration of macromolecules and suggested that enormously long capillary lengths are necessary for the concentration fields to achieve steady state. Similar results were also obtained by Cohen and Metzner [18] from a somewhat more rigorous analysis of the migration problem. In both cases, however, the flow field was taken to be independent of the concentration field.

In actual practice, however, the viscosity of a polymer solution is strongly dependent on the polymer concentration and hence any alteration in the concentration field is likely to affect the flow field quite significantly. Thus, it may be expected that the requirements of flow lengths suggested by the above analyses are somewhat exaggerated since the interdependence between viscosity and concentration has not been taken into account. In fact, Janssen [23] argues that owing to the severe coupling between the viscosity and the concentration, an instability mechanism somewhat analogous to 'thermal explosion due to viscous heating' will be operative and the concentration redistribution will be complete within a relatively short period. In support of this notion, Janssen referred to the observation of constant film thickness being attained within a short distance for falling film flows. However, we feel that this concept also represents another limiting case. Admittedly viscosity-concentration coupling will play an important role in promoting faster development of the migration process. However, the opposing Fickean diffusion flux is not likely to allow for such a runaway situation as proposed by Janssen. Janssen's analysis, which is valid for very dilute polymer solutions, essentially relates to fully developed conditions and provides a tool for the estimation of the detailed concentration profiles. An interesting feature of the analysis is that it predicts formation of a polymer free solvent layer once a critical wall shear stress is exceeded. Dutta and Mashelkar [24] have extended this analysis in order to demonstrate that it can serve as an upper bound of the migration effect for very dilute solutions.

Subsequently, the problem of capillary and falling film flows under fully developed conditions was examined carefully [13, 25]. The results obtained were consistent with the available experimental data in a sense that they served to provide upper bounds on the migration effects, where the lower bound was provided by the situation, when migration was absent. Interestingly, these fully developed concentration field (FDCF) asymptotes are unique for all capillary or film dimensions at a given solution concentration and imposed stress level.

Presently, there is no analysis available, which can enable an estimation of the order of flow times (or flow lengths) that will be necessary for appreciable migration to occur when there is a severe viscosity-concentration coupling. In the present work, an attempt has been made to provide some insight into this hitherto neglected aspect of the stress-induced migration phenomenon. Such a knowledge of flow times or lengths is not only of fundamental importance, but is a key towards assessing the extent of influence of migration phenomena on transport processes.

GOVERNING EQUATIONS

We consider the steady, incompressible flow of a polymer solution through a capillary tube. The concentration and the velocity fields at the point of entry to the tube are specified and we wish to determine the rearrangement of these two fields caused by the migration phenomenon. For this flow situation, the continuity equation is

$$\frac{1}{r}\frac{\partial}{\partial r}(rv_r)+\frac{\partial v_z}{\partial z}=0 \tag{1}$$

and the momentum equations can be written as

$$\rho\left(v_r\frac{\partial v_r}{\partial r}+v_z\frac{\partial v_r}{\partial z}\right)=-\frac{\partial p}{\partial r}+\frac{1}{r}\frac{\partial}{\partial r}(r\tau_{rr})+\frac{\partial \tau_{rz}}{\partial z} \tag{2}$$

$$\rho\left(v_r\frac{\partial v_z}{\partial r}+v_z\frac{\partial v_z}{\partial z}\right)=-\frac{\partial p}{\partial z}+\frac{1}{r}\frac{\partial}{\partial r}(r\tau_{rz})+\frac{\partial \tau_{zz}}{\partial z} \tag{3}$$

In addition, the polymer concentration (c) is governed by the following equation

$$v_r\frac{\partial c}{\partial r}+v_z\frac{\partial c}{\partial z}=-\frac{1}{r}\frac{\partial}{\partial r}(rJ_r)-\frac{\partial J_z}{\partial z} \tag{4}$$

The radial diffusion flux, J_r, comprises two contributions; one is the usual Fickean contribution arising out of a concentration gradient and the other is an entropic contribution resulting from gradients of the chemical potential function caused by the deformation induced free energy changes. Thus

$$J_r=-D_0\left(\phi\frac{\partial c}{\partial r}+c\frac{\partial F}{\partial r}\right) \tag{5}$$

where $\phi=\phi(c)$ is a correction factor accounting for the concentration depend-

ence of diffusivity [18]. The chemical potential function, F, is taken to be [18]

$$F = (\lambda\dot{\gamma})^2 - \tfrac{1}{2}\ln[1 + 2(\lambda\dot{\gamma})^2] \tag{6}$$

Equation (6), which is valid for dilute solutions, approximates the polymer molecules as linear dumbells [26]. The relaxation time, λ, is obtained from

$$\lambda = N_1/2\tau_{rz}\dot{\gamma} \tag{7}$$

where $N_1 = N_1(c, \dot{\gamma})$, $\tau_{rz} = \tau_{rz}(c, \dot{\gamma})$ and the shear rate, $\dot{\gamma}$, is defined as

$$\dot{\gamma} = [\tfrac{1}{2}(\boldsymbol{\Delta}:\boldsymbol{\Delta})]^{1/2} \tag{8}$$

The appropriate boundary conditions for this problem are as specified at the tube inlet (at $z = 0$), symmetry conditions at $r = 0$ and zero velocities and fluxes at the wall ($r = R$).

GENERAL FORMULATION

Equations (1) to (8) represent a set of coupled equations and their solution in the exact form presents formidable difficulties. However, for the problem considered by us, several simplifications can be made to facilitate a solution. Firstly, the variables are non-dimensionalized as follows:

$$\xi = r/R \qquad \zeta = z/L \qquad u = v_r/\varepsilon v$$
$$v = v_z/v \qquad \psi = p/p_{ns} \qquad \theta = c/c_0$$

and $\eta = \mu/\mu_0$. Equations (1) to (5) can now be written as follows

$$\frac{1}{\xi}\frac{\partial}{\partial\xi}(\xi u) + \frac{\partial v}{\partial\zeta} = 0 \tag{9}$$

$$\frac{\partial\psi}{\partial\xi} = \theta(Re\,\varepsilon) + \theta(\varepsilon^2) \tag{10}$$

$$\alpha\frac{\partial\psi}{\partial\zeta} = \frac{1}{\xi}\frac{\partial}{\partial\xi}\left(\xi\eta\frac{\partial v}{\partial\xi}\right) + v(Re\,\varepsilon) + v(\varepsilon^2) \tag{11}$$

and

$$Pe\,\varepsilon\left(u\frac{\partial\theta}{\partial\xi} + v\frac{\partial\theta}{\partial\zeta}\right) = \frac{1}{\xi}\frac{\partial}{\partial\xi}\left(\xi\phi\frac{\partial\theta}{\partial\xi} + \xi\theta\frac{\partial F}{\partial\xi}\right) + v(\varepsilon^2) \tag{12}$$

where $Pe = VR/D_0$, $\alpha = P_{ns}R^2/\mu_0 VL$, $Re = 2\rho VR/\mu_0$, and $\varepsilon = R/L$. Since for typical problems of interest the aspect ratio $\varepsilon \ll 1$ and also the Reynolds number is quite low (<1), we get $Re\,\varepsilon \ll 1$. Equations (9) to (12) can be simplified by neglecting the terms of the order of ε^2 and $Re\,\varepsilon$.

It is important to note here the difference between our solution and that provided by Cohen and Metzner [18]. Several simplifying assumptions have been made by Cohen and Metzner. These are (i) $\phi = 1$; (ii) $u = 0$, $v = v(\xi)$, i.e. velocities do not depend on the concentration, this implies neglecting of viscosity

concentration coupling; (iii) the chemical potential function depends on $\dot{\gamma}$ only and not on concentration, and (iv) the term $u(\partial\theta/\partial\xi)$ in Eq. (12) is neglected even though the above analysis shows that this term is of the same order of magnitude as the term $v(\partial\theta/\partial\zeta)$. In the following, however, none of these restrictive assumptions will be made and a more realistic solution will be obtained.

The appropriate boundary conditions for the Eqs. (9) to (12) can be prescribed as follows:

$$\zeta = 0, \quad \text{all } \xi, \quad \theta = \theta_0(\xi), \quad u = u_0(\xi), \quad v = v_0(\xi), \quad \psi = 1 \tag{13a}$$

$$\text{all } \zeta, \quad \xi = 0, \quad \frac{\partial\theta}{\partial\xi} = \frac{\partial v}{\partial\xi} = u = 0 \tag{13b}$$

$$\text{all } \zeta, \quad \xi = 1, \quad \phi\frac{\partial\theta}{\partial\xi} + \theta\frac{\partial F}{\partial\xi} = 0, \quad u = v = 0 \tag{13c}$$

$$\zeta = 1, \quad \text{all } \xi, \quad \psi = 0 \tag{13d}$$

Moreover, the shear gradient can now be approximated as

$$\dot{\gamma} = \frac{V}{R}\left[\left(\frac{\partial v}{\partial\xi}\right) + v(\varepsilon^2)\right] \tag{14}$$

Equation (10) implies that $\psi = \psi(\zeta)$ and therefore Eq. (11) can be integrated to give

$$v = \frac{\alpha}{2}\left(-\frac{d\psi}{d\zeta}\right)\int_{\xi}^{1}\frac{\xi^*\, d\xi^*}{\eta(\xi^*, \zeta)} \tag{15}$$

Note that the average velocity remains constant (see Eq. (20)), therefore Eq. (15) can be alternatively expressed as

$$v = \frac{1}{2B(\zeta)}\int_{\xi}^{1}\frac{\xi^*\, d\xi^*}{\eta} \tag{16}$$

where

$$B(\zeta) = \int_0^1 \xi^1 \int_{\xi^1}^{1}\frac{\xi^*\, d\xi^*}{\eta}\, d\xi^1 \tag{17}$$

The pressure profile can now be expressed as

$$\psi(\xi) = \frac{1}{\alpha}\int_{\zeta}^{1}\frac{d\zeta^*}{B(\zeta^*)} \tag{18}$$

and the radial velocity can be obtained from the axial velocity profiles by use of the continuity equation i.e.

$$u = -\frac{1}{\xi}\int_0^{\xi}\xi^*\frac{\partial v}{\partial\zeta}\, d\xi^* \tag{19}$$

Thus knowing the concentration profiles $\theta(\xi, \zeta)$ and hence $\eta(\xi, \zeta)$, Eqs. (17)

and (19) together allow determination of the velocity field, which in turn affects the θ-field (see Eq. (12)).

In addition to above, mass balance requirements dictate that

$$\int_0^1 \xi v \, d\xi = \tfrac{1}{2} \tag{20}$$

and

$$\int_0^1 \xi v\theta \, d\xi = \tfrac{1}{2} \tag{21}$$

The numerical solution must satisfy the above requirements.

Formulation for Power-law Liquids

Within the shear rate range of interest, the solution viscosity and the primary normal stress difference (N_1) can be adequately represented by a power-law behaviour. That is

$$\mu = K(c)\dot{\gamma}^{n(c)-1} \tag{22}$$

and

$$N_1 = A(c)\dot{\gamma}^{m(c)} \tag{23}$$

If the rheological parameters, K, n, A and m are also described by power-law relationships with concentration, such as

$$K = a_1 c^{b_1}, \qquad n = a_2 c^{b_2}, \qquad A = a_3 c^{b_3}, \qquad m = a_4 c^{b_4} \tag{24}$$

then

$$\lambda\dot{\gamma} = \frac{a_3}{2a_1} c^{b_3-b_1} \dot{\gamma}^{a_4 c^{b_4} - a_2 c^{b_2}} \tag{25}$$

and

$$\mu = K_0 (V/R)^{n_0 c^{b_2}-1} \left(\frac{\partial v}{\partial \xi}\right)^{n_0 c^{b_2}-1} \tag{26}$$

where $K_0 = a_1 c_0^{b_1}$ and $n_0 = a_2 c_0^{b_2}$. Note that when $b_2 \neq 0$ and $b_4 \neq 0$, normalization of μ and $\lambda\dot{\gamma}$ is not readily possible. However, if n and p are independent of concentration then

$$\mu_0 = K_0 (V/R)^{n-1} \tag{27}$$

$$\lambda\dot{\gamma} = \beta^* \theta^{b_3-b_1} \left(\frac{\partial v}{\partial \xi}\right)^{m-n} \tag{28}$$

where

$$\beta^* = We \Big/ \left(\frac{3n+1}{n}\right)^{m-n},$$

We being the Weissenberg number defined as

$$We = \lambda_{ns}\dot{\gamma}_{ns} = \frac{a_3}{2a_1} c_0^{b_3-b_1} \left(\frac{3n+1}{n}\frac{V}{R}\right)^{m-n} \tag{29}$$

Also, note that for power-law fluids the normalising parameter p_{ns} for pressure is the pressure drop in the absence of the migration effect and is given as

$$p_{ns} = \frac{2K_0 L}{R}\left(\frac{3n+1}{n}\frac{V}{R}\right)^n \tag{30}$$

and

$$\alpha = \frac{2(3n+1)}{n} \tag{31}$$

For polymer solutions whose rheological behaviour could be represented by power-law type of shear stress and first normal stress difference functions, an analysis of the (long) capillary flow problem entails solution of Eq. (12) using the velocity expressions given by Eqs. (16) and (19) and the relationships described by Eqs. (27) to (31). In the case when the viscosity and normal stresses are coupled with concentration ($b_1 \neq 0$, $b_3 \neq 0$, see Eq. (22)), the flow rate, Q, is expected to be greater than that predicted (Q_{ns}) from conventional no-slip theory. For a given flow rate, Q, this ratio then becomes

$$Q/Q_{ns} = [1/\psi(0)]^{1/n} \tag{32}$$

Clearly, when $b_1 = b_3 = 0$, the concentration and velocity fields are uncoupled and the ratio Q/Q_{ns} is unity.

Note that while performing the numerical calculations, a specific form of the function ϕ describing the concentration dependence of the diffusivity, that is $D = D_0\phi(c)$ is needed. Following Dutta and Mashelkar [13] we will take ϕ to be

$$\phi = 1 + \beta\theta \quad \text{where} \quad \beta = k_D c_0 \tag{33}$$

This form has been found to be reasonably valid for most dilute polymer solutions (27).

NUMERICAL METHOD

In order to obtain a clear understanding as to how the phenomenon of flow-induced polymer migration progresses in a capillary tube, the problem as formulated above was solved numerically using a finite difference method. Figure 1 shows a schematic of the numerical procedure adopted. At any given axial location, ζ (owing to the strong coupling between the concentration (θ) and the velocity (u, v) fields), an iterative scheme becomes necessary. Initially, at a given axial location ζ we assume certain θ, u, v, fields and then a new θ-field is obtained from a finite difference version of Eq. (12) written as follows:

$$-A_j\theta_{i,j+1} + B_j\theta_{i,j} - C_j\theta_{i,j-1} = D_j \tag{34}$$

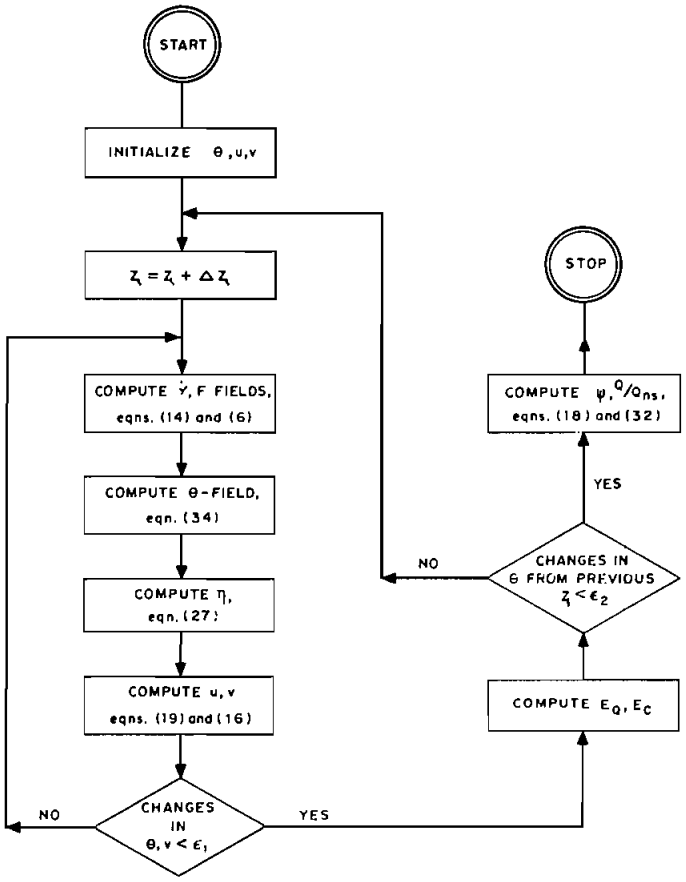

FIGURE 1 Flow chart of the numerical solution procedure.

where

$$h = 1/(JMAX - 1), \qquad g = 1/(IMAX - 1)$$

$$A_j = \bar{m}/2h^2 + \bar{n}/4h$$

$$B_j = \bar{m}/h^2 + \bar{o}/g - \bar{p}/2$$

$$C_j = \bar{m}/2h^2 - \bar{n}/4h$$

$$D_j = \theta_{i-1,j+1}A_j + \theta_{i-1,j}(\bar{o}/g + \bar{p}/2 - \bar{m}/h^2) + \theta_{i-1,j-1}C_j$$

$$\bar{m} = \phi, \qquad \bar{n} = \partial\phi/\partial r + \phi/r + \partial F/\partial r$$

$$\bar{o} = Pe\,\varepsilon v \quad \text{and} \quad \bar{p} = \frac{1}{r}\frac{\partial F}{\partial r} + \frac{\partial^2 F}{\partial r^2}$$

Note that in Eq. (34), $\bar{m}$, $\bar{n}$, $\bar{o}$, $\bar{p}$ are evaluated at the grid point i, j where $i = 1, 2, \ldots, IMAX$ indicates the location in the ζ direction and $j = 1, 2, \ldots, JMAX$ does so in the ξ direction. Equation (34) is in the familiar tridiagonal form. It can be solved easily under boundary conditions given by Eq.

(13) (b and c). Once θ-field is known, η is obtained from Eq. (27) and v and u-fields are then given by Eqs. (16) and (19), respectively. This procedure is continued until changes in θ and v fields between subsequent trials are less than ε_1. The calculations then proceed at the next axial location. If the changes in θ profiles between two consectuive axial locations are less than ε_2, then it is assumed that the process of concentration and velocity profile (in the coupled case) development are complete. Equations (18) and (32) are then used to obtain the pressure profile and the flow enhancement ratio.

Before proceeding with the actual calculations, numerical results were obtained to arrive at the appropriate grid sizes and the tolerance values. Table I illustrates the effect of grid spacing h on the numerical results. θ_0 and θ_w are the centreline and the wall concentrations at the axial location (ζ_d) where the development is complete. Clearly, as the grid spacing (h) is reduced the numerical solutions become more accurate as manifested by the reduction in errors associated with satisfying the balance Eqs. (20) and (21). However, beyond $JMAX = 21$ the improvement in accuracy is not commensurate with the increased computational effort. Similar exercises were undertaken to fix the values of $IMAX$, ε_1 and ε_2. All subsequent results were therefore obtained with $JMAX = 21$, $IMAX = 501$, $\varepsilon_1 = 0.1\%$ and $\varepsilon_2 = 0.01\%$.

In order to check the validity of the numerical scheme, results were obtained for a Newtonian liquid with concentration independent viscosity and relaxation time (λ), for which the chemical potential function is given as $F = (\lambda\dot{\gamma})^2$. Under fully developed conditions, the concentration profile for this model problem is given as [13]

$$\theta = \frac{\delta^4 \exp(-\delta^2\xi^2)}{2[\delta^2 + \exp(-\delta^2) - 1]} \tag{35}$$

where $\delta = \tau_w\lambda/\eta$. Figure 2 illustrates the concentration profiles at different axial locations. It is seen that the development is achieved at $\zeta = 0.32$ or $\zeta^* = \zeta/2\,Pe\,\varepsilon = 0.134$. More importantly, the numerically obtained fully developed concentration profile is in very good agreement with the exact results given by Eq. (35). For power-law fluids, our numerical results were compared with the

TABLE I

Effect of grid spacing on numerical results†

JMAX	θ_0	θ_w	ζ_d	e_q‡ (%)	e_c§ (%)
11	1.083	0.754	0.31	1.16	1.54
21	1.088	0.747	0.32	0.30	0.83
31	1.089	0.745	0.32	0.12	0.68
41	1.089	0.744	0.32	0.03	0.59

† $\varepsilon\,Pe = 2.682$, $We = 1.0$, $n = 0.424$, $m = 0.8$, $\beta = 0$, $b_1 = b_3 = 0$ (uncoupled), $IMAX = 101$, $\varepsilon_1 = 0.1\%$, $\varepsilon_2 = 0.2\%$.

‡ Error in satisfying Eq. (20) at $\zeta = \zeta_d$.

§ Error in satisfying Eq. (21) at $\zeta = \zeta_d$.

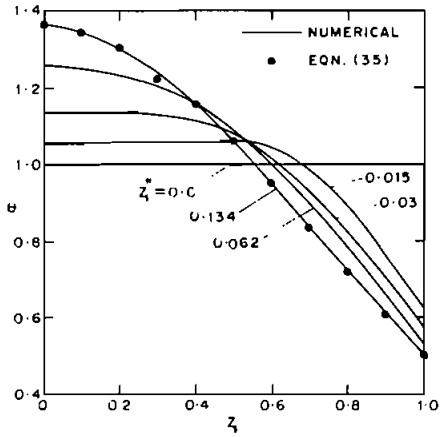

FIGURE 2 Comparison of concentration (——) numerical, (●) analytical for a Newtonian liquid. $F = (\lambda\dot{\gamma})^2$. $Pe\,\varepsilon = 1.188$, $We = 1.0$, $\beta = 0$, $m = 2$, $n = 1$, $b_1 = b_3 = 0$.

results reported by Cohen and Metzner [18]. Figure 3 shows the wall concentration as a function of the axial location for an uncoupled problem. Very sharp drop in the wall concentration within a very short flow length is quite evident. Also, it is seen that the numerical results are consistent with those reported by Cohen and Metzner. An exact correspondence between the two results, however, was not possible owing to some differences in the details of the problem formulation as discussed earlier.

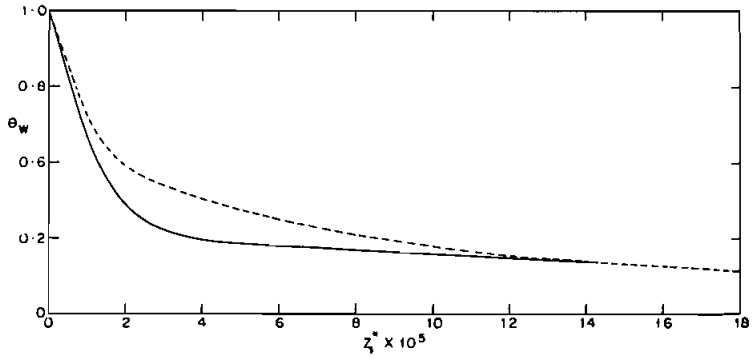

FIGURE 3 Comparison of wall concentration for $We = 3$, $Pe\,\varepsilon = 10.1$, $\beta = 0$, (——) present work with $m = 0.8$, $n = 0.424$, $b_1 = b_3 = 0$; (– – –) results reported by Cohen and Metzner [18].

RESULTS AND DISCUSSION

In the following, we shall present some numerical results in order to demonstrate the influence of the viscosity-concentration coupling on the migration behaviour. Meaningful results, however, were possible only within a certain parametric space only.

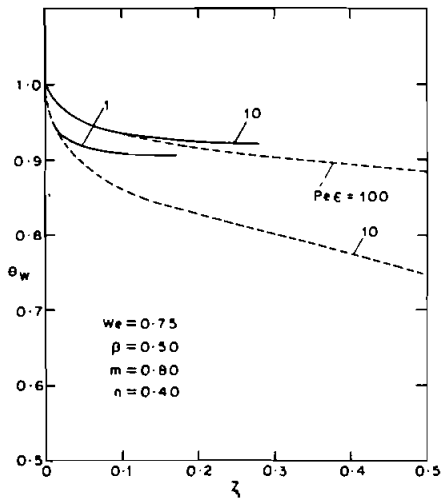

FIGURE 4 Variation of wall concentration with axial distance for different values of $Pe\,\varepsilon$. —— uncoupled case, – – – coupled case ($b_1 = 1.46$, $b_3 = 1.4$).

Since our primary interest is to ascertain the role of flow length and the polymer elasticity on the migration process, results were obtained for fixed values of β, m, and n. In particular, the values used were $\beta = 0.5$, $m = 0.8$, and $n = 0.4$. Besides, the initial concentration profile was assumed to be uniform ($\theta_0(\xi) = 1$) and the velocity profile $v_0(\xi)$ was taken to be identical to that in the absence of migration with $u_0(\xi) = 0$. Figure 4 shows the wall concentration of the polymer as a function of axial location. It is evident that for both the coupled and the uncoupled cases, bulk of the polymer depletion occurs very rapidly within a relatively short distance from the inlet followed by a much more gradual depletion. The extent of migration, however, depends strongly on the factor $Pe\,\varepsilon$, with the migration effect becoming more pronounced as $Pe\,\varepsilon$ decreases. Since the results are for constant We, decrease in $Pe\,\varepsilon$ is possible either due to higher diffusion coefficient (D_0) or longer flow length. Assuming that D_0 does not change, the results imply that increased capillary length is expected to lead to a more pronounced migration provided the equilibrium concentration profile is not reached. Also, the nature of concentration profile development and the extent of migration differ considerably for the coupled and the uncoupled case. When the velocity field is taken to be independent of the concentration profile, equilibrium is reached much faster. In the coupled case, the development of the concentration as well as the velocity fields is slower but the magnitude of the migration effect is considerably larger. This is rather unexpected and the reason for this is not clear at the moment although it is likely to be related to the severe coupling between the flow field and the concentration field.

The numerical results presented in Figure 4 suggest that for the real life situations, where the concentration and flow fields are interdependent, much longer flow lengths are necessary to reach equilibrium as compared to the idealised situation represented by an uncoupled case. However, it is interesting to

TABLE II

Effect of We on the migration effect for $Pe\,\varepsilon = 100$, $\beta = 0.5$, $m = 0.8$, and $n = 0.4$

We	θ_0	θ_w	Q/Q_{ns}	e_q, %	e_c, %
		Uncoupled Case ($b_1 = b_3 = 0$)			
0.1	1.000	1.000	1.000	—	—
0.5	1.000	0.992	1.000	—	—
0.75	1.001	0.955	1.000	0.13	0.13
1.00	1.005	0.870	1.000	0.13	0.11
2.00	1.070	0.404	1.000	0.13	0.51
		Coupled Case ($b_1 = 1.46$, $b_3 = 1.4$)			
0.10	1.000	1.000	1.000	—	—
0.50	1.000	0.991	1.018	0.15	0.13
0.75	1.002	0.853	1.150	0.17	0.03

note that to achieve an extent of migration ($\Delta\theta = \theta_0 - \theta_w$) which is identical to that in the uncoupled case, the flow length required for the coupled case is considerably less. In other words, a given extent of migration will be achieved in much smaller flow lengths as compared to that predicted from the analysis which neglects the severe coupling between the concentration and the flow field.

It is expected that more strongly elastic polymer solutions will have larger migration effect and naturally longer flow lengths will be necessary to achieve the equilibrium. Table II and Figure 5 illustrates just this behaviour. As before, in

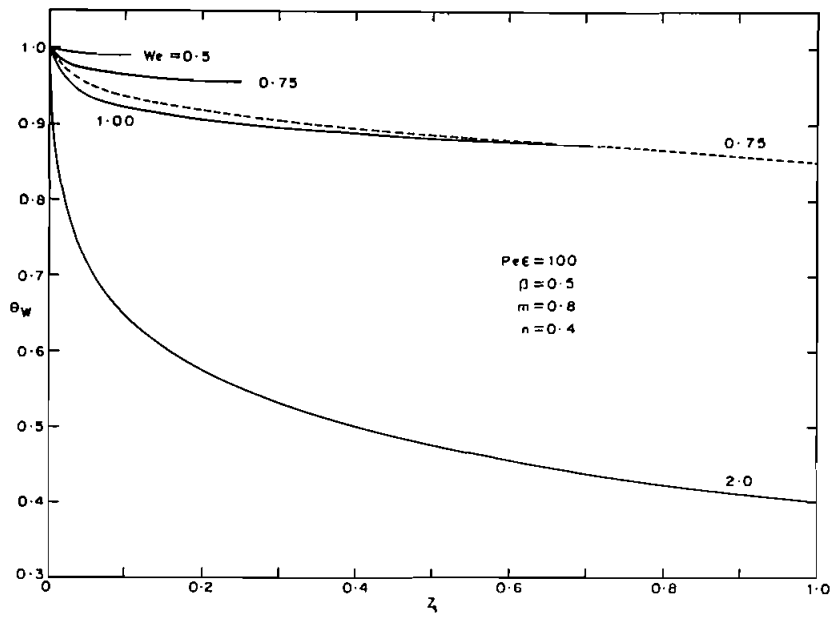

FIGURE 5 Variation of wall concentration with axial distance for different We values, —— uncoupled case, – – – coupled case ($b_1 = 1.46$, $b_3 = 1.4$).

comparison to the uncoupled case, incorporation of coupling leads to a much larger migration effect and significantly slower rate of development towards the equilibrium situation. However, the flow length required to achieve the same extent of migration is considerably less for the coupled case. For example, when $We = 0.75$ for the coupled case, the same amount of $\Delta\theta$ can be obtained in capillaries with lengths which will be about one-tenth of those applicable under uncoupled conditions. Also, note that the results presented in Figure 5 show that under coupled conditions, equilibrium is not reached for $We = 0.75$ within the flow length provided. Still, the extent of migration possible within this length was enough to lead to a 15% flow enhancement (see Table II). Thus, for the migration phenomenon to be manifested in appreciable flow enhancement, flow lengths considerably less than those required for equilibrium conditions may be quite adequate.

Influence of Macromolecular Migration on Heat and Mass Transport Processes

In the foregoing we have tried to assess the influence of macromolecular migration on the extent of flow enhancement. An important consideration relates to the influence of such migration effects on the net heat and mass transfer enhancement under such conditions. Mashelkar and Dutta [8] have addressed this problem. They used a simple phenomenological view point—in that they replaced the 'no slip' boundary condition by a 'slip' boundary condition and reexamined the problem of heat and mass transfer. They showed that in the high Peclet number region, where the heat and mass transfer resistance is confined to a very narrow zone near the solid wall, the influence of even a minor slip effect could be quite significant. Mashelkar and Dutta's effort had a limitation in view of the fact that a constant slip velocity, which was arbitrarily taken to be proportional to the wall shear stress (again assumed constant) was used to assess the influence of slip condition. In view of the more rigorous handling of the problem, it is no more necessary for us to use such *ad hoc* methods and a better appreciation of the influence of macromolecular migration could be obtained by using the numerical results presented here.

We consider the dissolution of a low molecular weight solute in a polymer solution, which is flowing through a capillary. We will essentially examine the enhancement of wall mass transfer coefficient within the framework of 'Leveque approximation'. If $\bar{k}_m$ is the average mass transfer coefficient in the entrance region in the presence of macromolecular migration and $\bar{k}$ is the one in its absence, then the ratio of the two could be simply worked out as

$$\frac{\bar{k}_m}{\bar{k}} \simeq \left(\frac{\dot{\gamma}_{wm}}{\dot{\gamma}_w}\right)^{1/3} = \left(\frac{n\dot{\gamma}_w^*}{3n+1}\right)^{1/3} \tag{36}$$

The above presupposes that the molecular diffusivity of the small molecular weight solute in the dilute polymer solution is practically independent of the polymer concentration, which seems to be a perfectly valid assumption (28).

Table III gives the values of k_m/k, which represents the mass transfer enhancement in the wall region due to macromolecular migration. It is readily

TABLE III

Effect of migration on enhancement of mass transfer coefficient ($We = 0.75$, $\beta = 0.5$, $n = 0.4$, $m = 0.8$)

	$Pe\,\varepsilon = 10$		$Pe\,\varepsilon = 100$	
ζ	$\dot{\gamma}_w^*$	$\bar{k}_m/\bar{k}$	$\dot{\gamma}_w^*$	$\bar{k}_m/\bar{k}$
0.00	5.5	1.0	5.5	1.0
0.05	6.82	1.074	6.16	1.0385
0.10	7.25	1.0965	6.42	1.053
0.15	7.51	1.1094	6.60	1.063
0.20	7.72	1.1197	6.74	1.070
0.25	7.91	1.129	6.85	1.076
0.30	8.08	1.137	6.95	1.081
0.35	8.25	1.145	7.03	1.085
0.40	8.41	1.152	7.11	1.089
0.45	8.59	1.160	7.19	1.0934
0.50	8.79	1.169	7.25	1.0965

seen that even though the extent of migration is somewhat marginal, the influence on the wall mass transfer coefficient is significant. This observation is important, since it implies that even when gross manifestations in terms of flow enhancement are not observable (due to only marginal extent of migration occurring in the entrance region) it is still adequate to cause enough alteration in the hydrodynamics in the concentration boundary layer and result in a significant enhancement in mass transfer. Many situations on mass and heat transfer analysed by Mashelkar and Dutta [8] appear to be those, where enough flow lengths (or times) may not have been provided for the equilibrium extent of macromolecular migration to be reached. However, the present work throws light on this apparent contradition and shows as to why significant heat/mass transfer enhancements would still be possible.

LIMITATION OF THE NUMERICAL PROCEDURE

Unfortunately, the present numerical method failed to yield meaningful results for *We* greater than unity and hence results on the extent of flow enhancement in the high *We* region could not be generated. This limitation also precluded any comparison of the numerical results with the experimental data reported by Cohen and Metzner [7]. The failure of the present approach at high *We* may be due to several reasons. One of the reasons is as follows. It was assumed by us that the inertial terms in Eqs. (10) and (11) were negligible since they were of the order of $Re\,\varepsilon$ and ε^2. Such an assumption is likely to be valid only at distances far away from the inlet ($\zeta = 0$). For small ζ, inertial effects may be important and neglecting this effect may lead to velocity and concentration profiles which are not meaningful.

The inadequacy of the chemical potential function given by Eq. (6) also needs to be commented upon. This expression based on the linear dumbell model, is

valid for dilute solutions at moderate deformation rates and may not truly represent the potential function at high *We* values.

CONCLUDING REMARKS

In the foregoing, an attempt has been made to study the process of stress-induced polymer migration in narrow capillaries by accounting for the severe interdependence between the flow and the resulting concentration fields. A simplified numerical procedure has been used. Two key points emerge from these numerical calculations. Firstly, to achieve a given extent of migration (flow enhancement ratio) the flow lengths required are considerably less than those predicted by the simplified (uncompleted) analysis, which have been presented in the literature in the past. Secondly, under equilibrium conditions, the migration effect is considerably more than that suggested by the simplified treatments and correspondingly the flow lengths required to attain such conditions are also significantly higher.

The numerical procedure developed by us suffers from several draw backs, the most important one being its inability to generate meaningful results for high *We*. Possible reasons for this have been outlined. In particular, it needs to be emphasized that a numerical procedure to obtain the solution of the governing velocity and concentration equations incorporating the inertial effects is necessary. This will also enable a better understanding of the role of the entrance region. In this work, at the capillary inlet, the polymer concentration profile was assumed to be uniform and the velocity field was taken to be that obtainable in the absence of migration. A more realistic starting point should be the incorporation of both uniform concentration and velocity fields. Such a situation cannot be handled with the numerical procedure developed here and it calls for an even more rigorous approach.

NOMENCLATURE

a_1, a_2, a_3, a_4	constants for rheological parameters
A	power law constant for normal stress difference
b_1, b_2, b_3, b_4	constants for rheological parameters
B	dimensionless pressure gradient
c	polymer concentration
c_0	initial polymer concentration
D_0	polymer diffusivity
F	chemical potential function
J_r	radial flux
J_z	axial flux

k_D	parameter controlling concentration dependence of polymer diffusivity
K	power-law constant for shear stress
L	capillary length
m	power-law index for normal stress difference
n	power-law index for shear stress
N_1	first normal stress difference
p	pressure
p_{ns}	pressure drop in absence of migration
Pe	Peclet number, VR/D_0
Q	volumetric flow rate
Q_{ns}	volumetric flow rate without migration
r	radial distance
R	capillary radius
Re	Reynolds number, $2\rho VR/\mu_0$
u	dimensionless radial velocity
v	dimensionless axial velocity
v_r	radial velocity
v_z	axial velocity
V	mean velocity
We	Weissenburg number
Z	axial distance

Greek letters

α	parameter defined in Eq. (31)
β	$k_D C_0$
β^*	parameter in Eq. (28)
$\dot{\gamma}$	shear rate
$\dot{\gamma}_w$	wall shear rate
$\dot{\gamma}_{wm}$	wall shear rate in the presence of migration
δ	$\tau_w \lambda/\mu_0$
$\dot{\gamma}_w^*$	$\dot{\gamma}_w R/V$
Δ	rate of deformation tensor
ε	R/L
ζ	dimensionless axial distance
ζ^*	$\zeta/z\, Pe\, \varepsilon$
η	dimensionless viscosity

θ	dimensionless concentration
θ_0	centreline concentration
θ_w	wall concentration
λ	relaxation time
μ	viscosity
μ_0	reference viscosity
ξ	dimensionless radial distance
ρ	density
$\boldsymbol{\tau}$	shear stress tensor
τ_w	wall shear stress
ϕ	function describing concentration dependence of diffusivity
ψ	dimensionless pressure

REFERENCES

1. Astarita, G., Marrucci, G., and Palumbo, G., *Ind. Eng. Chem. Fund.*, **3,** 333 (1964).
2. Carreau, P.J., Bui, Q.H., and Leroux, P., *Rheol. Acta,* **18,** 600 (1979).
3. Peev, G., and Nikolova, A., *J. Non. Newt. Fluid Mech.*, **8,** 319 (1981).
4. Popadic, V.O., *AIChE J.*, **21,** 610 (1975).
5. Therien, N., Coupal, B., and Corneille, J.L., *Can. J. Chem. Eng.*, **48,** 17 (1970).
6. Kozicki, W., Pasari, S.N., Rao, A.R., and Tui, C., *Chem. Eng. Sci.*, **25,** 41 (1970).
7. Cohen, Y., and Metzner, A.B., *J. Rheol.*, **29,** 67 (1985).
8. Mashelkar, R.A., and Dutta, A., *Chem. Eng. Sci.*, **37,** 969 (1982).
9. Dutta, A., and Mashelkar, R.A., *AIChE J.*, **29,** 519 (1983).
10. Dutta, A., and Mashelkar, R.A., *Rheol. Acta,* **21,** 52 (1982).
11. Dutta, A., and Mashelkar, R.A., *Chem. Eng. Commun.*, **16,** 361 (1982).
12. Dutta, A., and Mashelkar, R.A., *Chem. Eng. Commun.*, **33,** 181 (1985).
13. Dutta, A., and Mashelkar, R.A., *J. Non-Newt. Fluid Mech.*, **16,** 279 (1984).
14. Metzner, A.B. in Shah, D.O., and Schecter, R.S. (eds.), Improved Oil Recovery by Surfactant and Polymer Flooding, Academic Press, New York, 1977.
15. Tirrell, M., and Malone, M.F., *J. Polym. Sci., Polym. Ph. Ed.*, **15,** 1569 (1977).
16. Metzner, A.B., Cohen, Y., and Rangel-Nafaile, C., *J. Non-Newt. Fluid Mech.*, **5,** 449 (1979).
17. Cohen, Y., and Metzner, A.B., *AIChE. Symp. Ser.*, **212, 78,** 77 (1982).
18. Cohen, Y., and Metzner, A.B., *Rheol. Acta,* **25,** 28 (1986).
19. Aubert, J.H., and Tirrell, M., *J. Chem. Phy.*, **72,** 2694 (1980).
20. Aubert, J.H., Prager, S., and Tirrell, M., *J. Chem. Phys.*, **73,** 4103 (1980).
21. Cohen, Y., Ph.D. Thesis, University of Delaware, Newark, 1980.
22. Drout, R., and Maugin, G. A., *Rheol. Acta,* **22,** 336 (1983).
23. Janseen, L.P.B.M., *Rheol. Acta,* **19,** 32 (1980).
24. Dutta, A., and Mashelkar, R.A., *Rheol. Acta,* **22,** 455 (1983).
25. Dutta, A., and Mashelkar, R.A., *Chem. Eng. Comm.*, **39,** 277 (1985).
26. Peterlin, A., *Pure Appl. Chem.*, **12,** 563 (1966).
27. Vrentas, J.S., and Duda, J.L., *AIChE J.* **25,** 1 (1979).
28. Kulkarni, M.G., and Mashelkar, R.A., *Chem. Eng. Sci.*, **38,** 925 (1983).